Journal of Magnetic Resonance 201 (2009) 131–136

Contents lists available at ScienceDirect

Journal of Magnetic Resonance

journal homepage: www.elsevier.com/locate/jmr

# Aplicability of TNT "super-Q detection" to multipulse sequences

Alan Gregorovič *, Tomaž Apih

*Institute "Jožef Stefan", Solid State Physics, Jamova 39, 1000 Ljubljana, Slovenia*

ARTICLE INFO

*Article history:*
Received 24 June 2009
Revised 25 August 2009
Available online 6 September 2009

*Keywords:*
Nuclear quadrupole resonance
NQR
Trinitrotoluene
TNT
Multipulse sequences
Spin lock
Quality factor
Super-Q detection

ABSTRACT

The use of high-Q probes to increase the sensitivity in NMR and NQR is a well-known technique, however very high Q values are associated with several limitations. This paper explores the $^{14}$N NQR multipulse detection of trinitrotoluene (TNT) signal-to-noise ratio as a function of the pickup coil Q factor, with a particular emphasis on the "super-Q" regime, where probe bandwidth becomes narrower than the NQR linewidths. We have used a mixed experimental–theoretical approach to find the TNT Q-dependent signal-to-noise value which avoided the inconvenient construction of a probe at every Q. The process has been repeated for a range of excitation/detection frequencies and a 2D sensitivity map was obtained. Our analysis suggests, that sensitivity is maximum and practically Q-independent when $400 < Q < 4000$. However, because the conflicting requirements of the SLSE excitation and the "super-Q" detection, only a gain of $\sim 6$ dB is obtained compared to a conventional $Q \sim 100$ coil.



## 1. Introduction

One of the basic techniques to increase the sensitivity in nuclear magnetic resonance (NMR) and nuclear quadrupole resonance (NQR) is the use of a high-Q probe [1] consisting of a tuned pickup coil with a high quality factor Q, where the underlying assumption is sensitivity scaling with $\sqrt{Q}$. However, there is a practical limit of increasing Q beyond any measure, which is determined by the high-Q probe limitations. First, a high-Q probe has a very long dead-time, typically an order of magnitude longer than its characteristic time constant

$$\tau_c = \frac{Q}{\omega_0}, \tag{1}$$

where $\omega_0$ is the excitation/detection frequency. The problem is very pronounced at low $\omega_0$ and remedies in the form of active damping just after the RF pulse [2,3] are quite complicated. Second, the probe bandwidth is proportional to $\omega_0/Q$ and becomes very narrow at high Q, eventually, in the "super-Q" limit [4] even narrower than the resonance line under investigation. This results in a severe lineshape distortion. And finally, a high-Q probe is not easy to build. Conventional solenoid coils at RF frequencies have Q's around 100 [5]. This value can be optimized by an appropriate coil geometry, but the increase is modest. Another option, suitable only for low frequencies, is the use of a Litz wire, which increases Q by roughly a factor of two. Coils with a higher Q can be obtained with a superconductor [6,7], but with obvious difficulties.

There are however applications where the intrinsic sensitivity is so low, that dealing with the above nuisances can be acceptable. One of these is certainly the detection of explosives by $^{14}$N NQR [8,9]. The set of the NQR frequencies, which is defined by the electric field gradients at the site of $^{14}$N nuclei in the sample, serves here as a unique fingerprint to identify the material. Unfortunately, these frequencies tend to be very low, typically between 500 kHz and 5 MHz, resulting in a poor sensitivity. The already low sensitivity is then further reduced by the requirement of remote detection, e.g. the detection of buried landmines, or by a small filling factor, e.g. detection of explosives hidden in luggage. Nevertheless, the necessity for a reliable detection has in recent years seen the development of several techniques with enhanced sensitivity for NQR detection of explosives [10–20].

One of the recently investigated methods suitable for the detection of trinitrotoluene (TNT) is a combination of a multipulse sequence for excitation/detection and a matched filter (MF) [12]. The benefit of using a MF is its simplicity, which provides an easy way to optimize the detection sensitivity. For example, it was here predicted and experimentally confirmed that a spin-lock spin-echo (SLSE) pulse sequence [21]

$$90^\circ_{\pm y} - (\underbrace{\tau - 90^\circ_x - \tau}_{t_{seg}})_N \tag{2}$$

with a short repetition time $t_{seg}$ and consequently a low spectral resolution, produces a much higher sensitivity compared to a simi-

* Corresponding author.
*E-mail address:* alan.gregorovic@ijs.si (A. Gregorovič).

1090-7807/$ - see front matter © 2009 Elsevier Inc. All rights reserved.
doi:10.1016/j.jmr.2009.08.013

lar detection with a longer $t_{seg}$ and a high spectral resolution. Nevertheless, TNT NQR detection still requires further enhancements. A promising direction seems to be the "super-Q" detection [4], which we are exploring in this article.

We are confronted with two principal difficulties when "super-Q" detection is applied to TNT: the first is related to multiple closely spaced resonance lines in TNT, while the second to the short available acquisition time which is imposed by the multipulse sequence. Whereas closely spaced resonance lines can be considered only as a nuisance of finding the frequency yielding the best sensitivity, the short acquisition time severely undermines one of the key requirements for the effectiveness of the "super-Q" detection; acquisition time substantially longer than $\tau_c$. Because the construction of a "super-Q" probe is difficult, we first decided to estimate whether the sensitivity of a TNT multipulse "super-Q" detection is improved compared to a conventional detection and if the improvement is large enough to warrant the development of such a probe.

The paper is organized as follows: in Section 2 we first overview the principles behind a "super-Q" detection on an exponentially decaying signal. In the next step we extend the analysis to include the off-resonance excitation/acquisition and multipulse excitation with segmented acquisition, as appropriate for TNT. In the last part of this section we develop an algorithm to predict the TNT NQR response for an arbitrary $Q$ probe from an experimentally obtained TNT response with a chosen low-$Q$ probe. In Section 3 we present a two dimensional predicted TNT sensitivity $\omega_0 - Q$ map, which suggest the optimal range of $Q$ values and frequencies for maximum detection sensitivity. We also discuss the feasibility of optimal probe construction. In Section 4 we summarize our conclusions.

## 2. "Super-Q detection

"Super-Q" detection is in NMR/NQR defined by a much narrower probe bandwidth compared to the intrinsic linewidth of the resonance line under the investigation. Because of this, the acquired signal at the spectrometer becomes a band-limited version of the induced signal in the pickup coil. However, at the same time the observed signal amplitude becomes much higher due to a high $Q$, and a net sensitivity increase is experienced. This effect will now be quantified for several model signals by assuming a very common NQR detection circuit [22] as presented in Fig. 1.

### 2.1. Model detection circuit

The primary detection element is a pickup coil with inductance $L$ and resistance $R$, whose associated quality factor is $Q = \omega_0 L/R$. The precession of magnetization induces a voltage across the pickup coil which is here represented by a source $V_{\mathrm{in}}(t)$ in series with the coil. The resistor thermal noise is represented by a voltage source $V_{\mathrm{th}}(t)$, with $\overline{V_{\mathrm{th}}^2(t)} = 4kTR\Delta\nu$, where $\Delta\nu$ is the bandwidth of interest. The probe, consisting of the pickup coil and the two capacitors $C_t$ and $C_m$, has an overall impedance $Z(\omega)$ at frequency $\omega$. The capacitors are used for matching purposes and are assumed as noiseless. The preamplifier is connected directly to the probe and is modeled with four elements [23,24]: an ideal amplifier with voltage gain $G$, a parallel current noise source $I_n(t)$, a series voltage noise source $V_n(t)$, and a noiseless input impedance $Z_0$. The quantities $Z_0, I_n(t)$, and $V_n(t)$ define the probe optimal $Z(\omega_0)$, where sensitivity is maximal. Here, the preamplifier noise factor $F$, defined by the ratio of its input and output signal-to-noise value, is minimal. In our case, $F$ for uncorrelated noise sources is

$$F = 1 + \frac{\overline{V_n^2(t)} + \overline{I_n^2(t)}\,|\,Z(\omega_0)|^2}{4kT\Delta\nu\,\mathrm{Re}(Z(\omega_0))} \tag{3}$$

with a minimum value $F_{\min}$ when

$$Z(\omega_0) = \sqrt{\frac{\overline{V_n^2(t)}}{\overline{I_n^2(t)}}}. \tag{4}$$

The preamplifier and the probe are said to be noise matched. The other condition for optimal $Z(\omega_0)$ is maximum power transfer achieved when the preamplifier and the probe are impedance matched

$$Z(\omega_0) = Z_0^*. \tag{5}$$

In practice, the parameters $\overline{V_n^2(t)}, \overline{I_n^2(t)}$, and $Z_0$ can not be chosen independently so some compromise has to be made. For this analysis however, we will assume perfect noise matching as well as perfect impedance matching exactly at the excitation/detection frequency $\omega_0$ so that

$$Z(\omega_0) = Z_0 = \sqrt{\frac{\overline{V_n^2(t)}}{\overline{I_n^2(t)}}}. \tag{6}$$

If the preamplifier gain is sufficiently high, then we can neglect all noise sources in subsequent stages and the compound noise is specified with a single parameter $F_{\min}$, the preamplifier minimal noise factor or more commonly with its noise figure $NF = 10\log(F_{\min})$.

### 2.2. Signal

The signal of interest $V_{\mathrm{sig}}(t)$ is the voltage just before the ideal amplifier (see Fig. 1) and is related to the pickup coil voltage $V_{\mathrm{in}}(t)$. In NMR/NQR the linewidths are usually much smaller than $\omega_0$, so that to a good approximation the fast oscilating term $\exp(i\omega_0 t)$ can be removed with the introduction of $\widetilde{V}_{\mathrm{sig}}(t)$ and $\widetilde{V}_{\mathrm{in}}(t)$ via

$$V_{\mathrm{sig}}(t) = \widetilde{V}_{\mathrm{sig}}(t)\exp(i\omega_0 t) \tag{7}$$

$$V_{\mathrm{in}}(t) = \widetilde{V}_{\mathrm{in}}(t)\exp(i\omega_0 t). \tag{8}$$

The expression connecting the voltages $\widetilde{V}_{\mathrm{sig}}(t)$ and $\widetilde{V}_{\mathrm{in}}(t)$ simplifies to

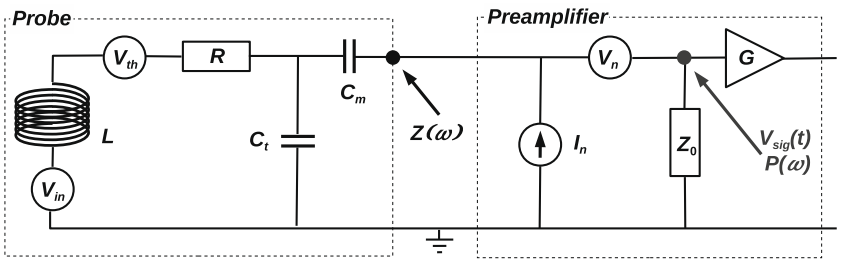


**Fig. 1.** Model detection circuit.

$$\widetilde{V}_{\mathrm{sig}}(t)+\frac{Q}{\omega_0}\frac{\partial}{\partial t}\widetilde{V}_{\mathrm{sig}}(t)=e^{i\varphi}\sqrt{\frac{QZ_0}{4\omega_0 L}}\widetilde{V}_{\mathrm{in}}(t) \tag{9}$$

where the phase $\varphi$ is not important for this discussion and therefore fixed at $\varphi=0$. The expression in Eq. (9) is derived with fundamental electric circuit analysis of our setup in Fig. 1 and by considering conditions from Eq. (6). While it is derived specifically for our setup, it should be valid more generally as it corresponds to an underdamped harmonic oscillator driven at its resonance frequency. The majority of NMR/NQR experiments are done in a regime where linewidths are much smaller than the probe bandwidth $\sim\omega_0/Q$ so that the contribution of $(Q/\omega_0)\frac{\partial}{\partial t}\widetilde{V}_{\mathrm{sig}}(t)$ in Eq. (9) can be neglected and the resonant circuit acts as an amplifier with gain $\sqrt{QZ_0/(4\omega_0 L)}$. No lineshape distortions occur in this case. In contrast, for high $Q$ values and especially in the "super-Q" regime, the term $(Q/\omega_0)\frac{\partial}{\partial t}\widetilde{V}_{\mathrm{sig}}(t)$ must be retained and has important consequences. For example, an induced on-resonance signal with a decay time $T_2^*$

$$\widetilde{V}_{\mathrm{in}}(t\geqslant 0)=\widetilde{V}_0\exp\left(-\frac{t}{T_2^*}\right) \tag{10}$$

and a maximum value of $\widetilde{V}_0$ at $t=0$ results in $\widetilde{V}_{\mathrm{sig}}(t)$ with a maximum value of

$$\widetilde{V}_{\mathrm{sig}}(t_{\mathrm{peak}})=\widetilde{V}_0\sqrt{\frac{QZ_0}{4\omega_0 L}}\left(\frac{\tau_c}{T_2^*}\right)^{\frac{\tau_c}{T_2^*-\tau_c}} \tag{11}$$

occurring at a delay

$$t_{\mathrm{peak}}=\frac{T_2^*\tau_c}{\tau_c-T_2^*}\ln\frac{\tau_c}{T_2^*}. \tag{12}$$

The instantaneous increase of $\widetilde{V}_{\mathrm{in}}(t)$ at $t=0$ is now replaced by a gradual increase, characterized by the coil's characteristic time constant $\tau_c$ as defined in Eq. (1). The peak is followed by a decaying part, which is now characterized by a decay time equal to the longest of $T_2^*$ and $\tau_c$.

### 2.3. Noise

The other quantity of interest is noise, again just before the ideal amplifier. Since it is a wide sense stationary process, it is best described with the power spectral density (PSD) function $P(\Delta\omega)=P_{\mathrm{th}}(\Delta\omega)+P_{\mathrm{n}}(\Delta\omega)$, where $\Delta\omega=\omega-\omega_0$ is the frequency offset between the frequency of interest $\omega$ and the probe tuning frequency $\omega_0$. Here $P_{\mathrm{th}}(\Delta\omega)$ is the contribution of the pickup coil resistance thermal noise, which is white at the origin, but the resonant circuit shapes it

$$P_{\mathrm{th}}(\Delta\omega)=\frac{kT}{1+\left(Q\frac{\Delta\omega}{\omega_0}\right)^2}. \tag{13}$$

The noise from sources $V_n(t)$ and $I_n(t)$ is shaped by the resonant circuit too, so that the preamplifier related noise $P_n(\Delta\omega)$ becomes

$$P_n(\Delta\omega)=(F_{\mathrm{min}}-1)\left(2-\frac{1}{1+(Q\frac{\Delta\omega}{\omega_0})^2}\right)kT. \tag{14}$$

The associated noise autocorrelation function is the inverse Fourier transform of $P(\Delta\omega)$

$$R_Q(\tau)=(2-F_{\mathrm{min}})\frac{\exp(-|\frac{\tau}{\tau_c}|)}{2\tau_c}kTZ_0+(2F_{\mathrm{min}}-2)\delta(\tau)kTZ_0, \tag{15}$$

where the second part includes the delta function $\delta(\tau)$ and the noise autocorrelation time $\tau_c$ is defined in Eq. (1). Here, the index $Q$ emphasizes the implicit $Q$-dependence of $R_Q(\tau)$ through the $Q$-dependence of $\tau_c$.

### 2.4. Signal-to-noise

We are now in a position to determine the signal-to-noise ratio $S/N$ for the detection of a particular signal. A simple and efficient method is the matched filter [4,12,25] (MF), which we use also here. Its maximum $S/N$ ratio for a discrete signal (which is also the maximum for any other linear filter) is defined as

$$\frac{S}{N}=\mathbf{s}^{\mathrm{T}}\cdot\mathbf{R}^{-1}\cdot\mathbf{s}, \tag{16}$$

where $\mathbf{s}$ is a vector representation of $\widetilde{V}_{\mathrm{sig}}(t)$ and $\mathbf{R}$ is the noise covariance matrix obtained with $\mathbf{R}=\langle\mathbf{n}\cdot\mathbf{n}^{\mathrm{T}}\rangle$. Here $\mathbf{n}$ are acquisitions obtained in exactly the same manner as $\mathbf{s}$ but containing only noise (sample removed), while the brackets represent an average over a large number of repeated experiments. Note that $S/N$ in Eq. (16) is defined in terms of power, instead of a more common NMR voltage definition, which is obtained by replacing $S/N$ with $(S/N)^2$. Whereas the two quantities differ by a square, their values become identical once expressed in dB units.

There is a useful simplification [4] of Eq. (16) for an ideal infinitely long acquisition or a real but long acquisition

$$\frac{S}{N}=\frac{1}{2\pi}\int_{-\infty}^{+\infty}\frac{S^*(\Delta\omega)S(\Delta\omega)}{P(\Delta\omega)}d\Delta\omega, \tag{17}$$

which avoids the need to invert $\mathbf{R}$. Here $S(\Delta\omega)$ is the Fourier transform of $\widetilde{V}_{\mathrm{sig}}(t)$ and long acquisition are defined as those where the total acquisition time significantly exceeds $\tau_c$ so that noise is well described by $P(\Delta\omega)$. It is now much easier to estimate the values of $S/N$ for the on-resonance signal from Eq. (10). The results for the parameters $T_2^*=1$ ms, $\widetilde{V}_0=1$ nV and $Z_0=50\,\Omega$ are shown in Fig 2. When the preamplifier is ideal, $NF=0$ dB and $S/N$ becomes a linear function of $Q$. It is interesting to note that $S/N$ linearly increases even when the probe bandwidth becomes much smaller than the signal linewidth. In the case of noisy preamplifiers, $NF>0$, the $Q$-dependence of $S/N$ splits into two regions: a probe limited regime at small $Q$ values, where $S/N$ still linearly increases with $Q$, and an amplifier limited regime at large $Q$ values, where $S/N$ becomes $Q$ independent. These results, originally derived by Suits et al. [4], suggest that increasing $Q$ for better sensitivity makes sense even for probe bandwidth's much smaller than the signal bandwidth, but when the preamplifier limited regime is reached, the gain becomes exceedingly small.

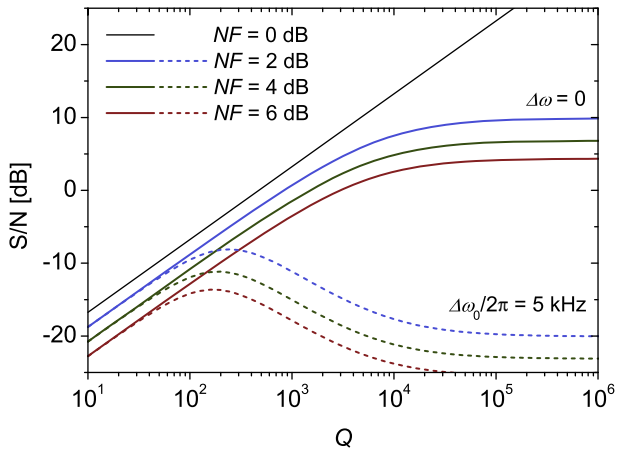


**Fig. 2.** Signal-to-noise dependence on the coil's quality factor $Q$ for a monoexponential decay on-resonance ($\Delta\omega_0=0$) and off-resonance by $\Delta\omega_0/2\pi=5$ kHz. The other numeric parameters used are $\widetilde{V}_0=1$ nV, $T_2^*=1$ ms, $\omega_{\mathrm{RF}}/2\pi=1$ MHz, $T=290$ K.

*2.4.1. Off-resonance*

When the induced signal is off-resonance by $\Delta\omega_0$ from the probe tuning frequency

$$\widetilde{V}_{\mathrm{in}}(t>0)=\widetilde{V}_0\exp(i\Delta\omega_0 t-\frac{t}{T_2^*}) \tag{18}$$

the $S/N$ $Q$-dependence changes in an interesting way as shown in Fig. 2. At low $Q$ values, there is practically no distinction between $\Delta\omega_0=0$ and $\Delta\omega_0\neq0$ cases, both linearly increse with $Q$. At intermediate $Q$ values the $S/N$ for the $\Delta\omega_0=0$ case still increases with $Q$, whereas it experiences a maximum for $\Delta\omega_0\neq0$ and then decreases upon further increase of $Q$. At high $Q$ values, both cases enter the preamplifier limited regime where $S/N$ is $Q$-independent, but for the $\Delta\omega_0=0$ cases this is the maximum $S/N$ value, whereas for $\Delta\omega_0\neq0$ this is not. It follows therefore, that using an extremely high $Q$ value for the detection of off-resonance signals will result in a poorer sensitivity than using a much lower but well determined value of $Q$ defined by the position of the $S/N$ maximum. This result is at first not truly surprising, because an off-resonance line is at low $Q$ values completely observed, whereas at high $Q$ values it is mostly unobserved. However, what is not so obvious is that here, because of the MF, this is only a consequence of the preamplifier noise. If the preamplifier is noiseless ($NF=0$) then the $S/N$ for on-resonance as well as for off-resonance detection are exactly the same, increasing indefinitely with $Q$ as seen of Fig. 2.

The existence of an optimal value of $Q$ for off-resonance detection was the primary motivation of this study. In samples with a single resonance line the choice of the excitation frequency and of the best $Q$ value is obvious; on-resonance detection with the highest achievable $Q$. However, in the case of several closely spaced resonance lines, already the choice of $\omega_0$ becomes non-obvious. Further, the position of the $S/N$ maximum will depend in a complicated way on both $\omega_0$ and $Q$. For any choice of $\omega_0$ and $Q$, some of the resonance lines might be detected on-resonance with a higher $S/N$ while several will be off-resonance with a lower $S/N$. The overall $S/N$ value will be determined by a particular combination of on/off-resonance conditions, as well as the intensities of the individual lines. And TNT is exactly such an example where for a mixture of the two crystallographic phases there are 12 $\nu_+$ resonance lines in the frequency range from 837 kHz to 871 kHz.

*2.4.2. Segmented acquisition*

The other difficulty in observing TNT with a "super-$Q$" probe is related to the exploitation of the spin-lock effect. Because the intrinsic sensitivity of TNT is very low, the signal is typically excited with a multipulse sequence, based on a SLSE sequence, and acquired in a segmented way as shown in Fig. 3a. In SLSE (see Eq. (2)) for example, a train of equally spaced $90^\circ_x$ pulses is applied after a preparatory $90^\circ_y$ pulse, so that an echo appears in each segment between two consecutive pulses. When $t_{\mathrm{seg}}$ is long compared

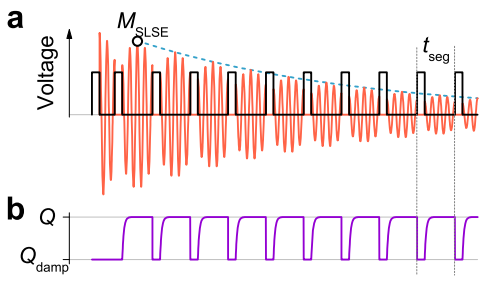


**Fig. 3.** A multipulse sequence acquisition scheme: (a) strong RF pulses and induced signal, (b) $Q$-switching between two values, the acquisition $Q$ and a fixed value for optimal damping $Q_{\mathrm{damp}}$.

to the echo decay time $T_2^*$, the echo amplitudes decay from segment to segment with a spin–spin relaxation time $T_2$ (an NQR analogue of the CPMG experiment). For shorter pulse spacings $t_{\mathrm{seg}}<T_2^*$ the echo amplitudes decay with a much longer decay time $T_{2,\mathrm{eff}}\gg T_2$, so that many more echoes can be accumulated. In TNT this decay time at room temperature is $T_{2,\mathrm{eff}}\sim80$ ms and allows for a significant increase of sensitivity. The downside of the method is that very long $T_{2,\mathrm{eff}}$ are obtained only with short $t_{\mathrm{seg}}$, so that the coil ring-down becomes a serious problem. An easy but partial solution to this problem is to use a permanently low-$Q$ probe, with obvious disadvantages. A much better approach is to use a $Q$-switching probe; with a high $Q$ between acquisition, and a low quality factor $Q_{\mathrm{damp}}$ during and right after the pulses as shown in Fig. 3b. Although having a low $Q$ during pulses is energy inefficient, this is essential if short $t_{\mathrm{seg}}$ are required. An example of the appropriate $Q$-switching design is described in Ref. [3], but we shall not go further into the details of $Q$-switching.

Segmented acquisition has two important consequences for the calculation of the $S/N$ ratio. First, at high $Q$ values the delay of the induced signal Eq. (12) becomes longer than the acquisition of a segment $t_{\mathrm{peak}}>t_{\mathrm{seg}}$ and much of the intensity slips out of our observation window. And second, noise correlation length $\tau_c$ eventually becomes longer than the segment acquisition length too, so that the acquisition is not long anymore and Eq. (17) is no longer appropriate. The $S/N$ has to be calculated with the original discrete expression Eq. (16) with the inconvenient inversion of the matrix $\mathbf{R}$.

The $S/N$ of the segmented acquisition will now be calculated numerically on a model signal. The model signal in the $m$th segment that captures the essentials of a multipulse TNT signal can be written as

$$\widetilde{V}_{\mathrm{in}}(t_{\mathrm{seg}}>t>0)=\widetilde{V}_0\exp\left(i\Delta\omega_0(t-\frac{1}{2}t_{\mathrm{seg}})-\frac{(m-1)t_{\mathrm{seg}}}{T_{2,\mathrm{eff}}}\right), \tag{19}$$

where $t$ is measured from the beginning of the $m$th segment, while the corresponding $\widetilde{V}_{\mathrm{sig}}(t)$ is again obtained with Eq. (9). The $T_2^*$ was here omitted, because it does not play a significant role. The noise covariance matrix $\mathbf{R}$ in Eq. (16) depends on a particular realization of the $Q$-switching circuit. To simplify the discussion, a simple form of $\mathbf{R}$ is here assumed which describes the basic idea and approaches the correct value for $t_{\mathrm{seg}}\gg\tau_c$. First, at extreme $Q$-values noise in neighboring segments is uncorrelated due to the $Q$-switching circuit so that $S/N$ from Eq. (16) is calculated with a sum across all the segments

$$\frac{S}{N}=\sum_{m=1}^{\infty}\mathbf{s}_m^{\mathrm{H}}\mathbf{R}_{\mathrm{seg}}^{-1}\mathbf{s}_m. \tag{20}$$

Here $\mathbf{s}_m$ is $\widetilde{V}_{\mathrm{sig}}(t)$ of the $m$th segment, while $\mathbf{R}_{\mathrm{seg}}$ is the segment noise covariance matrix. And second, $\mathbf{R}_{\mathrm{seg}}$ elements in $i$th row and $j$th column can be described by

$$\begin{aligned}&[\mathbf{R}_{\mathrm{seg}}]_{i,j}=R_Q((i-j)\Delta t);\quad i\neq j\\&[\mathbf{R}_{\mathrm{seg}}]_{i,i}=\tfrac{1}{\Delta t}\int_{-\frac{1}{2}\Delta t}^{+\frac{1}{2}\Delta t}R_Q(\tau)\,d\tau\end{aligned} \tag{21}$$

where $\Delta t$ is the sampling interval while $R_Q(\tau)$ is the autocorrelation function as defined in Eq. (15). When the signal from Eq. (19) is inserted in Eq. (20) we obtain an intermediate result involving only the first segment $\mathbf{s}_1$

$$\frac{S}{N}=2\frac{T_{2,\mathrm{eff}}}{t_{\mathrm{seg}}}\mathbf{s}_1^{\mathrm{H}}\mathbf{R}_{\mathrm{seg}}^{-1}\mathbf{s}_1. \tag{22}$$

We can further proceed only numerically, which we do so by using a typical set of values for TNT: $T_{2,\mathrm{eff}}=100$ ms, $t_{\mathrm{seg}}=1$ ms and $\widetilde{V}_0=1$ nV. The $S/N$ for two offsets and several $NF$ are shown in Fig. 4. The segmented acquisition as well as the long acquisitions

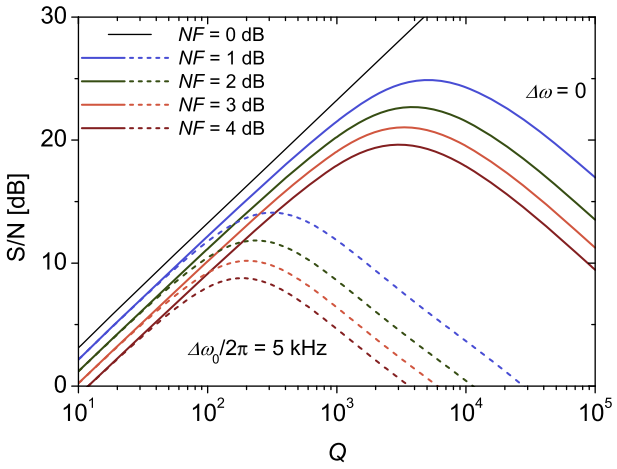


**Fig. 4.** Segmented acquisition signal-to-noise dependence on the coil's quality factor $Q$ for a monoexponential decay in the on resonance ($\Delta\omega_0 = 0$) and off resonance $\Delta\omega_0/2\pi = 5$ kHz case. The other numeric parameters used are $\widetilde{V}_0 = 1$ nV, $T_2^* = 100$ ms, $\omega_{RF}/2\pi = 1$ MHz, $T = 290$ K, and segment length $t_{seg} = 1$ ms.

from Fig. 2 for low $Q$ values behave similarly, $S/N$ is linearly proportional to $Q$. This is not surprising due to a short $\tau_c$ compared to the relevant acquisition time. However, at high $Q$ values and $NF > 0$, both on-resonance and off-resonance segmented $S/N$ decrease with $Q$ indefinitely, whereas the $S/N$ for a long acquisition always approaches a fixed nonzero value. We have thus found, that there is always an optimal $Q$ when segmented acquisition is used, and even more important using a higher $Q$ value will decrease the sensitivity, in strong contrast with a non-segmented acquisition.

### 2.5. Prediction of $S/N$ for TNT detection for an arbitrary $Q$

We will now consider the optimization of $S/N$ in the realistic case of TNT with 12 resonance lines. In TNT the induced signal in the $m$th segment is described by

$$\widetilde{V}_{in}(t) = \sum_{i=1}^{12} \alpha_i \exp\left(i(\omega_i - \omega_0)\left(t - \frac{1}{2}t_{seg}\right) - \frac{|\, t - \frac{1}{2}t_{seg}\,|}{T_{2,i}^*} - \frac{mt_{seg}}{T_{2,eff,i}}\right) \tag{23}$$

Here the $i$th $^{14}$N site is characterized by its resonance frequency $\omega_i$, amplitude $\alpha_i$, and decay times $T_{2,i}^*$ and $T_{2,eff,i}$. The parameters $\alpha_i$ and $T_{2,eff,i}$ depend on many parameters [26] related to the sample itself and to the particular pulse sequence parameters. These dependences are nontrivial and the values of $T_{2,eff,i}$ at arbitrary $\omega_0$ are difficult to predict. But, because $T_{2,eff,i}$ and $\alpha_i$ are both $Q$ independent a simple workaround exists for predicting the $S/N$ at an arbitrary $Q$ and $\omega_0$ which we describe in four steps. In the first step we record a SLSE TNT response for a preselected $t_{seg}$ and $\omega_0$ with a very low-$Q$ probe, so that the probe bandwidth is larger than the excitation bandwidth and the resonant circuit acts almost as a linear amplifier. These acquired signals incorporate all the necessary $\omega_0$ dependence of the parameters $\alpha_i$ and $T_{2,eff}$. In the second step, the $Q$-independent $\widetilde{V}_{in}(t)$ for every segment is determined from the measured $\widetilde{V}_{sig}(t)$ by using Eq. (9) and the probe $Q$ value. We obtain a reliable $\widetilde{V}_{in}(t)$ this way because probe bandwidth is much larger than the signal bandwidth. In the third step, we predict the $\widetilde{V}_{sig}(t)$ for a target $Q$ value, again with Eq. (9). We have here assumed a fixed dead time after the excitation pulse, which is characteristic of the quality factor during and right after the RF pulse. The corresponding $\mathbf{R}_{seg}$ is determined from $R_Q(\tau)$ with Eq. (21) where the target value of $Q$ is used. The last step consist of calculating the $S/N$ for the target $Q$ detection with Eq. (20), where $\mathbf{s}_m$ is now the vector representation of the calculated $\widetilde{V}_{sig}(t)$. The procedure is repeated for every $\omega_0$ value and a 2D $\omega_0 - Q$ map of sensitivity is produced.

## 3. Results and discussion

The experimental TNT NQR signal was obtained from 80 g of a commercial TNT powder, which was a mixture of 70% orthorhombic and 30% monoclinic phase. The SLSE pulse spacing was $t_{seg} = 540$ μs and all the pulses had the same length $t_{90} = 30$ μs. The phase of the first pulse was cycled between +Y and −Y while the phase of the other pulses was fixed +X. The receiver phase

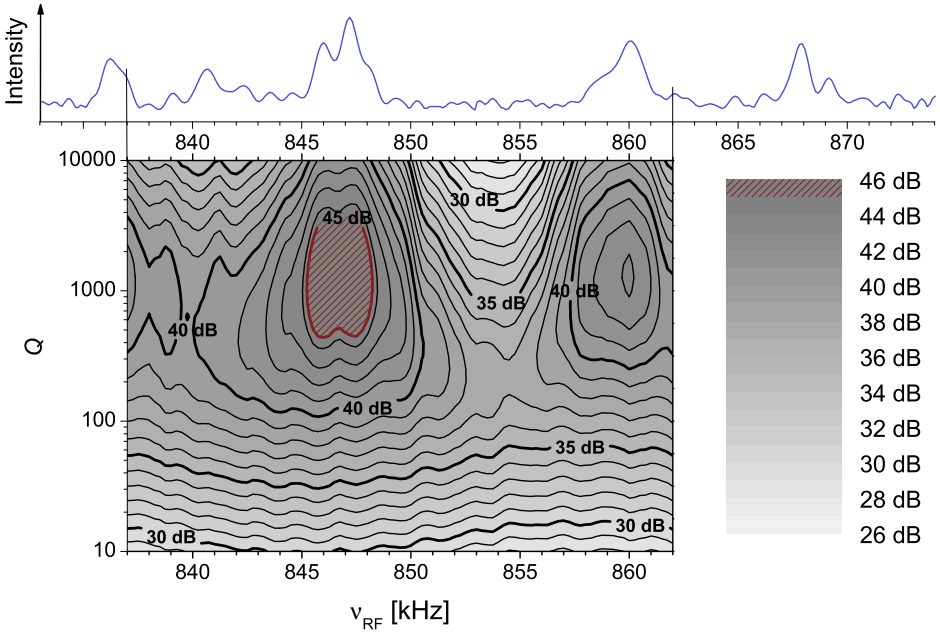


**Fig. 5.** Top: $^{14}$N TNT spectrum as obtained with a spin-echo pulse sequence. Bottom: A $\nu_{RF} - Q$ 2D map of the simulated $S/N$ for SLSE in TNT. The red region marks the optimal conditions.

was changed in accordance with the first pulse. A very low $Q = 34$ was used to increase the probe bandwidth beyond the excitation bandwidth. A very welcome side effect of a low-$Q$ probe, is its short dead time, which in our case was well below 100 μs. The preamplifier specified minimum noise figure is $NF = 1.3$ dB.

The results of the analysis from Section 2.5 are shown in Fig. 5 where the $S/N$ from Eq. (20) is calculated as a function of $Q$ and $\nu_{RF} = \omega_0/2\pi$. The region of maximum single-shot $S/N > 45$ dB is colored red. It changes little in a rectangular region spanning from 845—848 kHz and from $Q = 400$ to $Q = 4000$. While the frequency range of this region is not surprising because it coincides with several TNT frequencies, the $Q$ values certainly are. Obtaining a coil with a $Q = 4000$ is difficult and requires the use of a superconducting wire. On the other hand, a coil with a $Q \approx 400$ might be obtained much easier. Still, such a coil would require a very efficient $Q$-switching circuit.

A typical solenoid coil at the frequencies of 1 MHz has a $Q \sim 100$. The maximum $S/N$ obtained with such a coil would be 39 dB (see Fig. 5), or 6 dB less than, if the optimal $Q, 400 < Q < 4000$ probe is used. By comparison, for a non-segmented detection (see Fig. 2) on resonance, the difference between a $S/N$ of a $Q = 100$ probe and the optimal $Q$ probe with a $NF = 2$ dB amplifier is $\sim 20$ dB. Whereas the gain of 6 dB that we find for multipulse sequences is much smaller than the 20 dB for non-segmented acquisition, it certainly warrants the construction of a "super-$Q$" probe.

So far, the investigation considered only a single $t_{seg} = 540$ μs, which gives a very good $S/N$. It is reasonable to assume that an optimization of $t_{seg}$ would further increase $S/N$. However, because the $t_{seg}$ dependences of relaxation times $T_{2,eff,i}$ of the individual lines in TNT are not jet fully known, such an optimization would require a very time consuming repetition of our experimental procedure for every $t_{seg}$. Usually [21], two regions exist in a $t_{seg}$ dependence of $T_{2,eff}$: (i) a $t_{seg}$-independent region, or a "plateau" below a certain value of $t_{seg}$, and (ii) a $t_{seg}$-dependent region at longer $t_{seg}$, where $T_{2,eff}$ decreases steeply upon an increase of $t_{seg}$. In the "plateau" region the maximum $S/N$ increases with $t_{seg}$, however at the same time the position of the maximum shifts to a higher $Q$, which then implies a more demanding probe design. When $t_{seg}$ is further increased beyond the "plateau", $S/N$ may increase or decrease depending on the amount of $T_{2,eff}$ decrease. For even longer $t_{seg}, S/N$ will definitely decrease, approaching a value determined by a single long acquisition ($t_{seg} \to \infty$). Our preliminary results suggest that $t_{seg} = 540$ μs as used here is still in the $t_{seg}$-dependent regime, so that an additional increase of $S/N$ is most probably obtained with a shorter $t_{seg}$.

A potential pitfall of our algorithm in calculating the $S/N$ $Q$-dependence is the unknown form of the covariance matrix Eq. (21). So far, we have not been able to find any information about noise correlations for $Q$-switching devices, whereas, the construction of our $Q$-switching circuit is still in progress. Nevertheless, in our opinion, the primary reason for a low sensitivity increase we observe is the incompatibility of "super-$Q$" detection with spin-echo spin-locking techniques, rather than a poorly approximated noise covariance matrix.

Finally, we should here stress that the single-shot detection with a $S/N = 45$ dB, as found here, is very high, but it is obtained with a prepolarization unit [14,27], which increases the magnetization of every acquisition by approximately 30 dB. In experiments without prepolarization, the maximum value of TNT $S/N$ would be 15 dB, which is still above the limit for a reliable detection ($\sim 10$ dB [28]), and even allows for some further reduction of signal, either due to a smaller sample or greater sample-detector distance.

## 4. Conclusions

In conclusion, our results suggest that the optimal conditions for a SLSE TNT detection with $t_{seg} = 540$ μs are found when the excitation/detection frequency is between 845 and 848 kHz while the optimal $Q$ factor is between 400 and 4000. In this region the $S/N$ variation is smaller than 1 dB and offers good stability also in cases of temperature drift. While the optimal frequencies we find are not surprising, it is certainly interesting, that the optimal $Q$ values are as low as 400. These values make the "super-$Q$" probe and the necessary $Q$-switching device quite achievable. However, we should stress, that because of conflicting requirements of SLSE and "super-$Q$", the maximum gain that one may hope to obtain for TNT is about 6 dB compared to a typical $Q = 100$ probe.

## References

[1] A. Abragam, Principles of Nuclear Magnetism, Oxford University Press, New York, 2002.
[2] D.I. Hoult, Rev. Sci. Instrum. 50 (1979) 193.
[3] A.S. Peshkovsky, J. Forguez, L. Cerioni, D.J. Pusiol, J. Mag. Res. 177 (1) (2005) 67.
[4] B.H. Suits, A.N. Garroway, J.B. Miller, J. Mag. Res. 132 (1) (1998) 54.
[5] D.I. Hoult, R.E. Richards, J. Mag. Res. 24 (1976) 71.
[6] Y. Kondo, J.H. Koivuniemi, J.J. Ruohio, V.M. Ruutu, M. Krusius, Czech. J. Phys. 46 (1996) 2843.
[7] Q. Ma, IEEE Trans. Appl. Superconduct. 9 (1999) 3565.
[8] A.N. Garroway, M.L. Buess, J.B. Miller, J.B. Suits, A.D. Hibbs, G.A. Barrall, R. Matthews, L.J. Burnett, IEEE Trans. Geosci. Rem. Sens. 39 (6) (2001) 1108.
[9] J.A.S. Smith, R.M. Deas, M.J. Gaskel, Nuclear quadrupole resonance detection of landmines, in: H. Sahli, A.M. Bottoms, J. Cornelis (Eds.), International Conference on Requirements and Technologies for the Detection, Removal and Neutralization of Landmine and UXO, vol. 2, Vrije Universiteit, Brussels, Belgium, 2003, p. 715.
[10] A. Jakobsson, M. Mossberg, M.D. Rowe, J.A.S. Smith, IEEE Trans. Geosci. Rem. Sens. 43 (11) (2005) 2659.
[11] M. Nolte, A. Privalov, J. Altmann, V. Anferov, F. Fujara, J. Phys. D: Appl. Phys. 35 (9) (2002) 939.
[12] A. Gregorovič, T. Apih, J. Mag. Res. 198 (2009) 215.
[13] S.-K. Lee, K.L. Sauer, S.J. Seltzer, O. Alem, M.V. Romalis, Appl. Phys. Lett. 89 (21) (2006) 214106.
[14] J. Lužnik, J. Pirnat, V. Jazbinšek, T. Apih, A. Gregorovič, R. Blinc, J. Seliger, Z. Trontelj, Appl. Phys. Lett. 89 (2006) 123509.
[15] V.T. Mikhaltsevich, T.N. Rudakov, Phys. Stat. Sol. (b) 241 (2) (2004) 411.
[16] J.B. Miller, B.H. Suits, A.N. Garroway, J. Mag. Res. 151 (2) (2001) 228.
[17] D.Y. Osokin, R.R. Khusnutdinov, Appl. Magn. Reson. 30 (1) (2006) 7.
[18] D.W. Prescott, O. Olmedo, S. Soon, K.L. Sauer, J. Chem. Phys. 126 (20) (2007) 204504.
[19] T.N. Rudakov, Phys. Lett. A 358 (4) (2006) 322.
[20] K.L. Sauer, B.H. Suits, A.N. Garroway, J.B. Miller, Chem. Phys. Lett. 342 (3-4) (2001) 362.
[21] R.A. Marino, S.M. Klainer, J. Chem. Phys. 67 (7) (1977) 3388.
[22] J. Mispelter, M. Lupu, A. Brigut, NMR Probeheads for Biophysical and Biomedical Experiments, Imperial College Press, London, 2006.
[23] H.A. Haus, R.B. Adler, Circuit Theory of Linear Noisy Networks, The MIT Press, New York, 1959.
[24] F.N. Trofimenkoff, D.H. Treleaven, L.T. Bruton, Int. J. Circ. Theor. App. 2 (1973).
[25] Wikipedia, Matched filter—Wikipedia, The Free Encyclopedia, 2009. http://en.wikipedia.org/w/index.php?title=Matched_filter.
[26] A. Gregorovič, T. Apih, J. Chem. Phys. 129 (2008) 214504.
[27] J. Lužnik, J. Pirnat, V. Jazbinšek, T. Apih, R. Blinc, J. Seliger, Z. Trontelj, J. Appl. Phys. 102 (8) (2007).
[28] A.D. Hibbs, Alternatives for Landmine Detection, RAND, Santa Monica (CA), USA, 2003, Ch. Nuclear Quadrupole Resonance, p. 170. http://www.rand.org/pubs/monograph_reports/MR1608/MR1608.appj.pdf.